Concentration and stable carbon isotopic composition of ethane and benzene using a global three-dimensional isotope inclusive chemical tracer model

Alexandra Thompson and Jochen Rudolph
Centre for Atmospheric Chemistry, Chemistry Department, York University, Toronto, Ontario, Canada

Franz Rohrer and Olaf Stein
Institut für Chemie und Dynamik der Geosphäre II, Troposphere, Forschungszentrum Juelich, Juelich, Germany

Received 26 August 2002; revised 14 February 2003; accepted 21 March 2003; published 1 July 2003.

[1] A three-dimensional global chemical tracer model of the atmosphere has been adapted to include the stable carbon isotopic composition and isotopic fractionation of ethane and benzene. For computational efficiency the chemistry was based on a prescribed OH-radical concentration field, and therefore the feedback of ethane and benzene chemistry on the atmospheric OH-radical concentrations was not considered. The Emission Database for Global Atmospheric Research (EDGAR) V2.0 emission database used needed to be scaled by a factor of 2.22 in order to have good agreement between observed and modeled concentrations. Modeled isotopic compositions were consistent with the few published observations. The global distribution of modeled stable carbon isotope ratios and the derived mean photochemical ages of ethane and benzene are presented. The model predicts distinct regimes of photochemical aging and air mass mixing for polar regions. *INDEX TERMS:* 0365 Atmospheric Composition and Structure: Troposphere—composition and chemistry; 0368 Atmospheric Composition and Structure: Troposphere—constituent transport and chemistry; 1040 Geochemistry: Isotopic composition/chemistry; *KEYWORDS:* stable carbon isotope ratios, nonmethane hydrocarbons, ethane, benzene, mean photochemical age

Citation: Thompson, A., J. Rudolph, F. Rohrer, and O. Stein, Concentration and stable carbon isotopic composition of ethane and benzene using a global three-dimensional isotope inclusive chemical tracer model, *J. Geophys. Res.*, *108*(D13), 4373, doi:10.1029/2002JD002883, 2003.

1. Introduction

[2] Atmospheric nonmethane hydrocarbons (NMHC) have been the subject of numerous studies, mainly owing to their importance in the chemistry of the lower atmosphere. However, more recently they have also been studied with the intent to better understand the processes determining their atmospheric distribution. Because of the wide range of atmospheric lifetimes, sources that are nearly exclusively found only at the surface, and the primary loss process being reaction with OH-radicals, NMHC are useful as tracer species to investigate transport and mixing processes, as well as OH-radical initiated reactions in the atmosphere. In particular, NMHCs have been used to determine the extent of photochemical aging, via so-called "Hydrocarbon Clock" methods [*McKeen et al.*, 1990, 1996; *McKenna et al.*, 1995; *McKenna*, 1997; *Parrish et al.*, 1992; *Roberts et al.*, 1984; *Rudolph and Johnen*, 1990]. These methods determine the so-called photochemical age of an air mass by comparing the concentration ratio of two compounds with similar atmospheric lifetimes (for example n- and i-butane) as the ratio changes over time. However, the technique is only valid when certain assumptions are met [*Rudolph and Johnen*, 1990] and the results are not always robust when applied to an air mass consisting of parcels with significantly different photochemical ages [*Rudolph and Czuba*, 2000; *McKeen et al.*, 1996], which is the usual "real world" scenario. With the recent development of a method to measure the stable carbon isotope ratio of NMHC at atmospheric concentrations [*Rudolph et al.*, 1997], several isotopic studies of ambient NMHC have been carried out [*Rudolph et al.*, 1997; *Tsunogai et al.*, 1999; *Saito et al.*, 2002]. This has led to the development of the "Isotopic Hydrocarbon Clock" concept [*Rudolph and Czuba*, 2000]. In this method the change in the ratio of unlabeled (containing only ^{12}C atoms) to labeled (containing one ^{13}C atom) concentrations (i.e., the isotopic composition) of a compound is studied instead of the concentration ratios of chemically different compounds. The generally very small differences between rate constants of labeled and unlabeled NMHC for their reaction with OH-radicals [*Rudolph et al.*, 2000] allows the linearization of the exponential dependence between NMHC concentration ratios and the determination of a meaningful average age of NMHC [*Rudolph and Czuba*, 2000]. In this paper we present results of global-scale model calculations of the stable carbon isotope ratios of benzene and ethane.

0148-0227/03/2002JD002883

[3] We have chosen to focus on ethane and benzene in this paper for several reasons. The global distribution of the ethane concentration has been reasonably well characterized by measurement [*Rudolph*, 1995], due in part to its relatively long lifetime and subsequent high ambient concentrations and relatively uniform atmospheric distribution. The average benzene concentrations are not so well defined, mainly owing to its shorter atmospheric lifetime, which is approximately only 1/5th of the lifetime of ethane. However, for the same reason, observations of benzene concentration and isotope ratios represent considerably smaller temporal and spatial scales. Nevertheless, the atmospheric abundance of benzene is generally sufficient to allow measurement of concentration even in very remote locations [e.g., *Clarkson et al.*, 1996]. Finally, the kinetic isotope effect (KIE) for the reaction of benzene with OH-radicals was measured to be 7.5 ± 1.0‰ [*Rudolph et al.*, 2000]. It is expected that the effect of a KIE of this magnitude will clearly be visible in atmospheric measurements [*Rudolph and Czuba*, 2000; *Rudolph et al.*, 2000]. Although the KIE for ethane is presently unknown, published KIEs of reaction with the OH-radical of methane [*Saueressig et al.*, 2001] and other light alkanes [*Rudolph et al.*, 2000] allow us to make a plausible estimate of the KIE for ethane. In addition preliminary results of measurements of the ethane KIE (R. S. Anderson, York University, Canada, personal communication, 2002) indicate that this KIE is in the range 4–8‰.

[4] Ethane and benzene are removed from the atmosphere solely by destruction via OH-radical reaction and their atmospheric reactions only have a minor feedback on the atmospheric OH-radical concentration. This allows us to use a computationally very economic chemical tracer model, with a prescribed OH-concentration field to calculate the stable carbon isotope ratios of atmospheric ethane and benzene. The results of this simple isotope inclusive chemical tracer model (I^2CTM) are used to illustrate how knowledge of the isotopic composition and concentration of NMHC allows for differentiation between atmospheric dilution or mixing processes and photochemical aging.

2. Model Description

[5] The isotopic inclusive chemical tracer model (I^2CTM), solves the continuity equations for chemically reactive species over a global three-dimensional grid. The I^2CTM was adapted from *Prather et al.* [1987]. In this study each grid box covers 4° in latitude and 5° in longitude. There are nine vertical layers in the model, from the Earth's surface to 10 hPa, each level on average centered at the pressures of 959, 894, 787, 635, 470, 322, 202, 110, and 40 hPa. The I^2CTM uses a split operator method to separately calculate the effects of dynamic tracer redistribution, large-scale diffusion, chemistry, and emissions. The model was run for 4 years until the seasonal variation was in steady state from year to year. This paper discusses results from the surface layer only.

[6] The dynamic tracer redistribution processes (advection, wet and dry convection) are calculated every 8 hours. The advective transport of tracers in the model is based on the formulation of *Prather et al.* [1987]. Details of the treatment of convection processes are described by *Kraus et al.* [1996]. The meteorological data used are from the Goddard Institute for Space Sciences general circulation model, the GISS GCM II [*Hansen et al.*, 1983]. This data set contains 8-hour averages of mass flux, pressure fields, and convection frequencies, as well as 5-day averages of temperature and detailed convection statistics for one year.

Table 1. Summary of Total Annual VOC Emissions From the EDGAR V2.0 Database

Main Source	Total Annual Global Emission, Tg/year	
	Ethane	Benzene
Gas production and transmission	1.83	–
Oil production and transmission	1.36	0.02
Other fossil fuel combustion	0.72	1.27
Biofuel combustion	1.84	1.85
Large-scale biomass burning	1.17	1.38
Waste treatment	1.28	1.27
Total	8.20	5.79

[7] The model chemistry includes only removal of the tracer species via reaction with OH-radicals. The OH-radical concentration is prescribed by a time-dependent three-dimensional field taken from *Spivakovsky et al.* [2000]. Products, secondary reactions, and feedback mechanisms were ignored, simplifying the model and thus substantially reducing computational efforts. The chemistry in the model is calculated every hour.

[8] Emissions of ethane and benzene are introduced into the appropriate surface level model boxes on an hourly basis. The global distribution and strengths of the sources of NMHC are taken from the EDGAR V2.0 database [*Olivier et al.*, 1996]. EDGAR V2.0 characterizes emissions from up to 14 different sources types for ethane and benzene. For this work all sources are summed to create a single global emission distribution for each compound. Total annual global emissions for the main source categories as defined by the database are shown in Table 1. Emission rates were held constant throughout the year.

[9] The ratio of ^{13}C to ^{12}C is usually expressed in units of per mil (‰) relative to a reference:

$$\delta^{13}C = \frac{\left(\frac{[^{13}HC]}{[HC]}\right)_{sample} - \left(\frac{[^{13}C]}{[^{12}C]}\right)_{reference}}{\left(\frac{[^{13}C]}{[^{12}C]}\right)_{reference}} * 1000. \quad (1)$$

Here [HC] and [^{13}HC] is the concentration of the unlabeled and labeled hydrocarbon respectively. The standard reference is Vienna Peedee belemnite (VPDB). In order to calculate the stable carbon isotope ratios, two model runs were performed for each compound. The model was run using the rate constant for the compound containing only ^{12}C atoms (unlabeled, k_{OH}), as well as with the rate constant for reaction of compounds containing one ^{13}C atom (labeled, $^{13}k_{OH}$). Otherwise identical conditions were used. The relationship between the two rate constants is usually expressed in the form of the ratio of the two rate constants, $k_{OH}/^{13}k_{OH}$, the kinetic isotope effect (KIE). Since the difference between the two rate constants is generally extremely small the KIE is often expressed as per mil:

$$\varepsilon_{OH}(‰) = \left((k_{OH} - {}^{13}k_{OH})/k_{OH}\right) * 1000. \quad (2)$$

The rate constants used in this study were 2.57×10^{13} $cm^3 molecules^{-1} s^{-1}$ for ethane [*Atkinson*, 1994] and 1.18×10^{12} $cm^3 molecules^{-1} s^{-1}$ for benzene [*Semadeui et al.*, 1995]. The rate constant for the reaction of ^{13}C labeled compounds can be calculated rearranging (2):

$$^{13}k_{OH} = k_{OH} * (\varepsilon_{OH}/1000 - 1). \quad (3)$$

There are no published measurements of the KIE for the reaction of ethane with OH-radicals. Based on estimates of the ethane ε_{OH} derived from KIEs for the reaction of other alkanes with OH [*Rudolph et al.*, 2000] and recent, unpublished measurements that indicate that this value is in the range of 4–8‰ (R. S. Anderson, York University, Canada, personal communication, 2002) we use a value of 5‰. The ε_{OH} for benzene has been measured to be 7.5 ± 1.0‰ [*Rudolph et al.*, 2000].

[10] The difference in stable carbon isotope ratio between emission and observation for any given point in time and space can be calculated from modeled concentrations for the unlabeled and labeled compound ([HC] and [^{13}HC] respectively), according to the following equation:

$$\delta_s - \delta_a(‰) = \left([^{13}HC]/[HC] - 1\right) * 1000, \quad (4)$$

where δ_s is the isotopic composition of the hydrocarbon at the time of emission, and δ_a is the isotopic composition for the selected point.

[11] In order to derive stable carbon isotope ratios comparable to ambient measurements we therefore have to consider the stable carbon isotope ratio of the sources, δ_s. For these model calculations we assumed that there is no temporal or spatial variability of the isotopic composition of the emissions. *Rudolph et al.* [2002] and *von Czapiewski et al.* [2003] report stable carbon isotope ratios relative to VPBD for several NMHC from transportation related sources and biomass burning. On the basis of their findings, we use the average value of −28‰ for both ethane and benzene.

3. Results and Discussion

[12] Since there are very few ambient measurements of stable carbon isotope ratios of ethane or benzene available for comparison with the model results, we first compare the concentrations predicted by our model with published measurements.

3.1. Comparison of Modeled Concentrations With Observations

[13] The comparison of predictions from large-scale tracer models with atmospheric observations of NMHC mixing ratios requires an observational data set which is representative on the temporal and spatial scale used for modeling in order to avoid bias due to subscale processes [*Goldstein et al.*, 1995]. In the case of ethane such a data set exists. The latitudinal and seasonal dependence of the atmospheric mixing ratio of ethane has been determined by *Rudolph* [1995] from a set of 1500 observations in the remote troposphere. Comparing the averages for each month and 5° latitude band we find very good linear correlation between observation and model (observation = (2.22 ± 0.02) * Model Result) with a correlation coefficient $R^2 = 0.92$ (Figure 1). Despite being a factor of 2 too low, the model reproduces the shape of observed latitudinal distributions and seasonal variations well (Figures 2 and 3). This indicates that the EDGAR V2.0 database underestimates the strength of the various sources but that, in the case of ethane, the source distribution (spatial and temporal) is a realistic approximation.

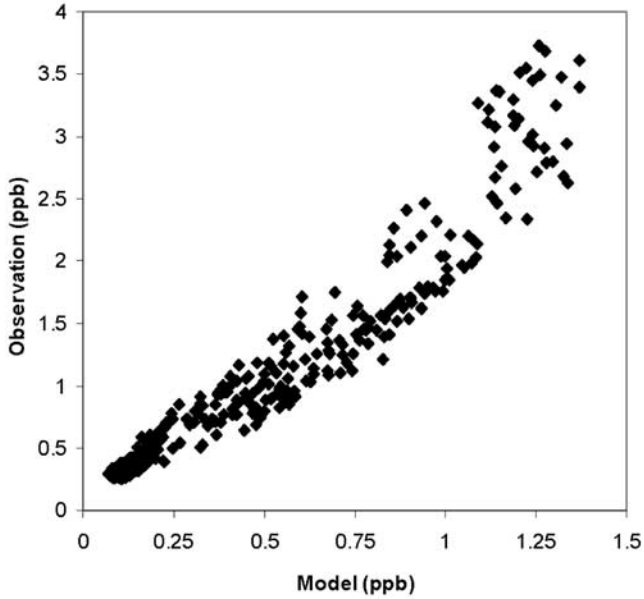

Figure 1. Comparison between model results and observations [*Rudolph*, 1995] of ethane concentration averages for each month taken over a 5° latitude band.

[14] Rudolph calculates the total ethane source strength to be 15.5 ± 6 Tg/year, which is supported by independent estimates of ethane emission rates [*Rudolph*, 1995]. The total annual ethane emission included in the EDGAR V2.0 database is 8.2 Tg/year, roughly a factor of 2 lower. In order to have agreement between model and observation, for this paper ethane emissions have been scaled by a factor of 2.22. This is also consistent with other estimates of the global ethane source strength; e.g., *Ehhalt* [1999] estimates that the total global source strength is 19 Tg/year. The EDGAR V2.0 database does not include any ethane emissions from vegetation or the oceans, estimated to be 5 Tg/year and 1 Tg/year respectively [*Ehhalt*, 1999]. However, these emissions are expected to have very different global distributions than the emissions considered in the model. Consequently ethane emissions from vegetation or the ocean are not entirely compatible with the good agreement between modeled and measured latitudinal and seasonal dependence of the atmospheric ethane concentration. Therefore it is not obvious whether the underestimation of the global ethane source strength in the EDGAR V2.0 database is due to an underestimation of the strength of individual source types or the absence of specific types of emissions.

[15] The observational database suitable for comparison with model predictions of the atmospheric mixing ratios of benzene is very limited. There is no globally complete distribution of benzene presently available, although there have been a number of studies of the benzene concentration

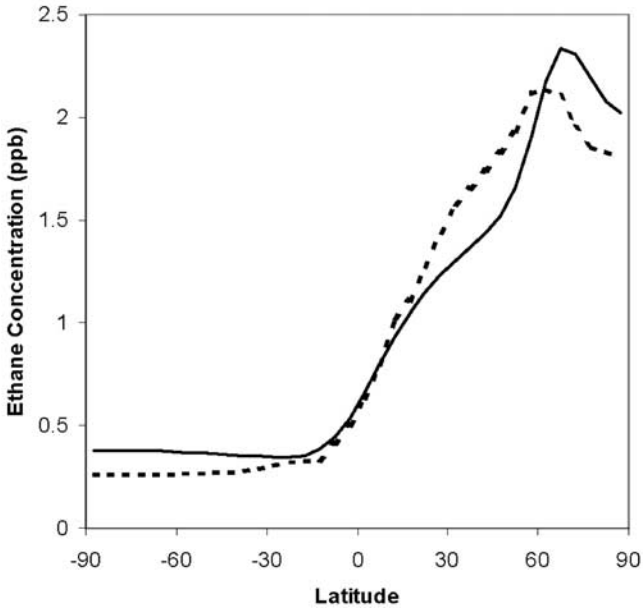

Figure 2. Annual average of ethane concentrations as a function of latitude for scaled model results (see text, dashed line) and observations (*Rudolph* [1995], solid line).

in the remote troposphere [e.g., *Greenberg and Zimmerman*, 1984; *Greenberg et al.*, 1990; *Gautrois*, 1999; *Singh et al.*, 1996; *Laurila and Hakola*, 1996; *Boudries et al.*, 1994; *Penkett et al.*, 1993; *Blake et al.*, 1996, 1997; *Clarkson et al.*, 1996]. With the inherent problem of comparing spot observations with monthly averages representative for an area of 4° in latitude and 5° in longitude and the paucity of data particularly in the Southern Hemisphere it is difficult to determine the accuracy of the I^2CTM model for benzene. Our comparison is based on data from remote areas, which will minimize the impact of nearby emissions but this does

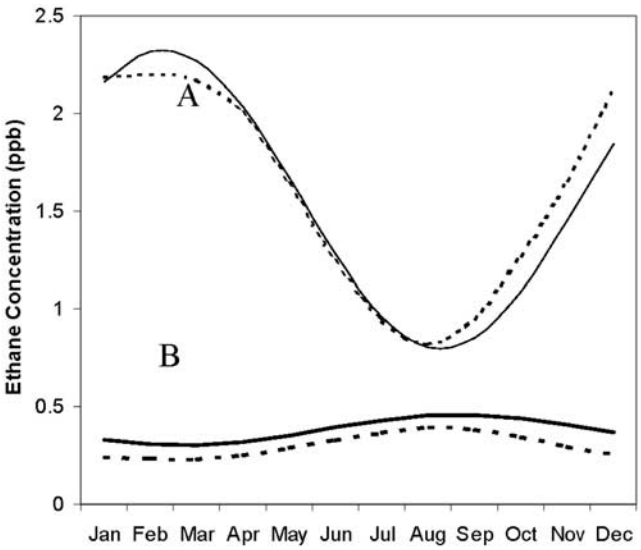

Figure 3. Seasonal variation of ethane concentration for (a) Northern Hemisphere and (b) Southern Hemisphere of scaled model results (see text, dashed line) and observations (*Rudolph* [1995], solid line).

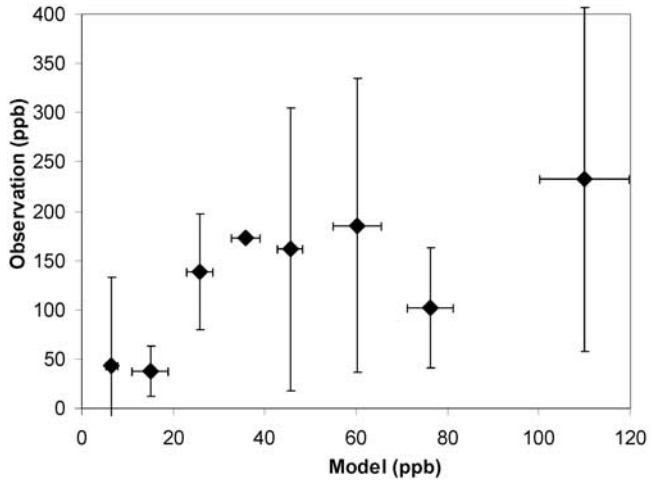

Figure 4. Comparison between model results and observations (see text for source) of benzene concentration. Diamonds and bars show average and ±1 SD for data binned by 5° latitude band and month.

not eliminate the uncertainty owing to the high variability of the tropospheric benzene concentration and the limited number of observations as evidenced by the high statistical uncertainty of the averaged observations (Figures 4 and 5). Even so, correlation of the above studies with the corresponding model results, show a slope (observations/model) of 2.4 ± 0.4, however only with a correlation coefficient (R^2) of 0.2 (Figure 4).

[16] In a comparison of modeled and observed NMHC mixing ratios for a continental site at middle to northern latitudes *Goldstein et al.* [1995] found that global tracer models are able reproduce the shape of observed seasonal cycles, although on an absolute-scale model and observations showed substantial differences. *Gautrois* [1999] observed the concentrations of both ethane and benzene over a seven year period at Alert, a remote site in the Arctic. Comparing these observations with I^2CTM results for both ethane and benzene at this site results in good linear correlations (both R^2 = 0.8), and slopes (observations/

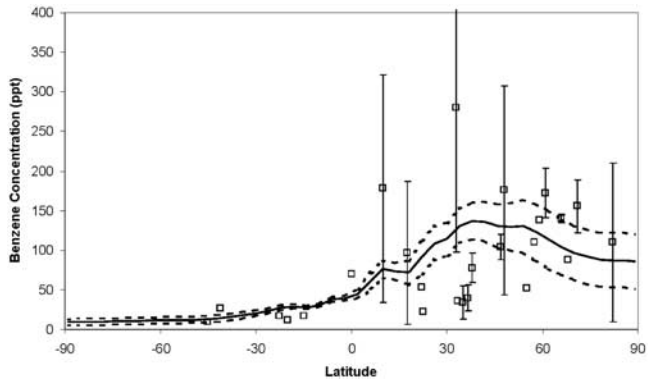

Figure 5. Benzene concentration as latitudinal band averages of scaled model (see text, solid line, ±1 SD dashed line) and observations (see text for sources, open boxes and vertical bars show average and range at that latitude).

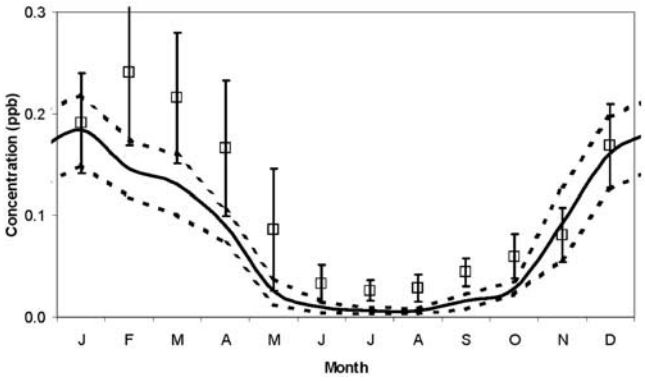

Figure 6. Benzene concentrations at Alert of scaled model (solid line, ±1 SD dashed line) and observations (*Gautrois* [1999], open boxes, vertical bars show ±1 SD).

model, monthly averages) of 2.3 and 2.4 for ethane and benzene respectively.

[17] The most likely explanation for a good agreement in the shape of seasonal cycles but major differences in absolute values is an incorrect estimate of the source strength. Total benzene emissions in the EDGAR V2.0 database are 5.8 Tg/year. *Ehhalt* [1999] estimated total annual benzene emissions to be 8 Tg. These comparisons suggest that, like ethane, benzene emissions in the EDGAR V2.0 database are too low. For this work we have scaled the benzene emissions by the factor of 2.22, which was also used for ethane. The latitudinal variation of the scaled benzene concentration is shown in Figure 5. The modeled seasonal variations of scaled benzene concentrations at Alert are compared with observations in Figure 6. The scaled benzene concentrations show reasonable agreement with observations.

3.2. Model Uncertainties

[18] Uncertainties in the I^{2}CTM arise in two areas: uncertainties affecting the accuracy of concentration and the stable carbon isotope ratios, and uncertainties affecting only the isotopic composition. In the first instance there are uncertainties in the OH field, k_{OH}, transport, and the strength and distribution of emissions. The accuracy of predicted isotopic compositions is also dependant on the uncertainty of the source composition, and the accuracy of the KIE. Additionally, the uncertainty of predicted isotopic compositions is dependant on the uncertainty in the relative distribution of emissions, but not the absolute values, i.e., scaling of the total emission strength does not effect δ_s-δ_a.

[19] *Spivakovsky et al.* [2000] estimates the uncertainty in the [OH] field to be 10–15% and the uncertainty in k_{OH} is 15% and 30% for ethane [*Atkinson*, 1994] and benzene [*Semadeui et al.*, 1995]. The consequences of uncertainty in transport or emission distributions are difficult to quantify. However, the good agreement of ethane concentration between model and observations indicate that the model realistically describes the most important transport processes as far as ethane is concerned. Although this gives some confidence that the description of transport processes is adequate for benzene, we have to consider that owing to the shorter atmospheric residence time of benzene, the temporal and spatial variability of the benzene concentration is significantly higher than for ethane. Therefore the results for ethane are not necessarily representative for benzene, especially if processes are considered that will primarily result in short term variations. Averaging over longer time periods, e.g., the use of monthly means, reduces this problem as long as the relevant processes result in linear dependencies.

[20] Owing to the limited amount of available measurements of the stable carbon isotopic composition of NMHC emissions the uncertainty of δ_s is difficult to assess. The combustion of biomass contributes 38% of total ethane emissions according to the EDGAR V2.0 database. *Von Czapiewski et al.* [2003] found the stable carbon isotope ratios of NMHC emitted by burning wood to differ by less than 4‰ from the parent fuel, (composition −26.7‰). *Rudolph et al.* [1997] found that ethane emitted from burning manuka (a native New Zealand plant) has a $\delta^{13}C$ of −28.7 ± 0.8‰. Both of these studies involved C-3 plants only. Emissions due to the combustion of C-4 plants can be expected to be substantially heavier. Their parent material composition is on average −13‰, [*Boutton*, 1991]. If the isotopic fractionation during combustion of C-4 plants is similar to that of C-3 plants, ethane emitted from C-4 combustion would be about 13‰ to 15‰ heavier than emissions from C-3 plants. C-4 biomass burning contributes 13% to the total global ethane emissions [*Lobert et al.*, 1999; *Greenberg and Zimmerman*, 1984]. This creates an average difference in δ_s of about 2‰. This difference will be higher for areas with high intensities of burning of C-4 plants such as savannas, and lower for areas with mainly C-3 type vegetation such as boreal plants.

[21] According to the EDGAR V2.0 database losses of natural gas during production and transmission contribute 22% of total ethane emissions. The $\delta^{13}C$ of ethane in natural gas has been found to range from −37‰ to −32‰ [*Fuex*, 1977], and −34.5‰ to −26.6‰ [*Jenden and Kaplan*, 1986].

[22] One fourth of the total ethane emissions in the EDGAR V2.0 database are due to fossil fuel usage and oil production. Crude oil has a stable carbon isotopic composition of −23‰ to −33‰ [*Yeh and Epstein*, 1981]. In two separate studies *Rudolph et al.* [1997, 2002] found the isotopic composition of alkanes in samples taken from transportation related sources to be on average −27.3‰ (SD 3‰) and −27.7‰ (SD 1.7‰).

[23] The other sources of ethane considered (∼15% of the total) include landfills, solvents, and waste treatment. There is nothing known about the stable carbon isotopic composition of emissions from these sources.

[24] Benzene emissions considered in this work comprise biomass burning (56%), fossil fuel combustion (22%), and waste treatment, landfills and solvents (22%). *Von Czapiewski et al.* [2003] found the stable carbon isotopic composition of benzene emitted by burning wood to be −25.5‰ to −27.5‰. Similar to ethane, this value is for the burning of C-3 plant material and on a global scale the contribution from C-4 plants has to be considered. Since benzene from C-4 biomass burning comprises 22% of the total biomass burning benzene emissions [*Lobert et al.*, 1999; *Greenberg and Zimmerman*, 1984] this may cause up to 3‰ difference in the global δ_s. The average isotopic composition of benzene emitted from transport related sources is −27.9‰

[*Rudolph et al.*, 2002]. We use a δ_s of −28‰ for both ethane and benzene, which is consistent with our present knowledge but only based on a limited number of studies.

[25] In this work we assumed no seasonal or spatial variability of the stable carbon isotopic composition of emissions. Owing to the lack of data it is difficult to quantify the uncertainty in this assumption. Since the emissions of two major sources (fossil fuel combustion and biomass burning) show little isotopic fractionation from the parent material, seasonal variation of a particular source is unlikely. The only major sources that we know to have an isotopic composition significantly different from other sources is natural gas ethane emissions and emissions from Savanna burning, which includes the burning of significant amounts of C-4 plants. According to the EDGAR V2.0 database, the spatial distribution of natural gas sources is similar to fossil fuel combustion in general. Savanna burning differs in seasonal and spatial dependence from other types of biomass burning. Since the contribution of burning C-4 plants to the global budgets of ethane or benzene is relatively small (see above) on a global scale we could expect an impact of 2−3‰ owing to this isotopically heavy source. However, on a local or regional scale this may be of considerable importance. Presently, available data does not suggest that spatial variability in the average isotopic composition of emissions will have a significant impact on ambient stable carbon isotope ratios of ethane or benzene, however the available database is very limited.

[26] Finally, there is uncertainty associated with the KIE. The ε_{OH} for benzene reacting with OH has been measured to be 7.5 ± 1.0‰ [*Rudolph et al.*, 2002]. The ε_{OH} for ethane is presently unknown. *Saueressig et al.* [2001] measured the ε_{OH} of methane to be 3.9 ± 0.4‰. *Rudolph et al.* [2000] measured the ε_{OH} of other light alkanes and used extrapolation arguments to estimate that the ethane ε_{OH} is probably 4−5‰. Preliminary experimental results agree that the ethane ε_{OH} is in the range 4−8‰ (R.S. Anderson, York University, Canada, personal communication, 2002). The temperature dependence of ε_{OH} has been ignored, however preliminary results show that within ambient tropospheric temperature ranges ε_{OH} for reaction of alkanes and aromatic compounds do not vary more than the experimental uncertainty (R.S. Anderson, York University, Canada, personal communication, 2002).

3.3. Global Distributions of Stable Carbon Isotope Ratios

[27] The global distribution of the stable carbon isotopic composition of ethane predicted by the I^2CTM is shown in Figure 7. There are clear isotopic composition gradients seen in the equatorial region during the northern winter months that are weakening during May to August. Pronounced seasonal variation of isotopic composition can be seen in the polar regions, where ethane is heavier during summer and lighter during winter. At high northern latitudes during winter the isotope ratios are close to the source composition of −28‰. In the remote southern hemisphere the stable carbon isotope ratios of ethane are relatively uniform, particularly from November until February. In general, higher stable carbon isotope ratios are found in remote areas, reflecting the higher extent of atmospheric processing (see 3.4).

[28] There are few published observations of the isotopic composition of atmospheric ethane in the literature. A comparison of published atmospheric ethane $\delta^{13}C$ measurements and model results is shown in Figure 8. *Tsunogai et al.* [1999] measured the isotopic composition of atmospheric ethane to be between −22‰ and −25‰ in the western North Pacific in March. Subsequently *Saito et al.* [2002] found this range to be −19‰ to −26‰ in the same region during May. The model predictions are in complete agreement with these observations.

[29] *Tsunogai et al.* [1999] also found that the isotopic composition of ethane became heavier over the open ocean compared to urban and coastal areas of Japan, consistent with the higher degree of processing for remote marine air. Their range of −25‰ to −28‰ over the urban and coastal parts of Japan does not agree with the model, which predicts a heavier ethane isotopic composition. As the model does include ethane emissions from the Japanese mainland (of −28‰) this discrepancy is likely due to the poor spatial resolution of the model, i.e., the instantaneous mixing of fresh emissions with a large amount of background air mass within the model box.

[30] *Rudolph et al.* [1997] measured the isotopic composition of ethane to be −22‰ and −29.7‰ with respective concentrations of 150 ppt and 250 ppt in two samples taken at Baring Head, a clean air site in New Zealand. Model results are consistent with the first data point, however the latter sample is of significantly lighter composition and higher concentration than predicted by the model for this site. Again, this inconsistency is probably due to the limited spatial resolution of the model and may reflect the possible impact of local or regional sources on the measurement.

[31] The stable carbon isotopic composition distribution of benzene (Figure 9) shows a significantly higher variability than the ethane distribution. This is a result of both the higher reactivity of benzene with respect to OH (the rate constant of benzene is almost five times greater than for ethane reacting with OH), and the higher ε_{OH}. Very high benzene isotopic composition gradients are found close to source areas, for example off the west coast of India during summer, off the northern east coast of South America, and in the Pacific Ocean close to southeast Asia. Similar to ethane, the model predicts the central Pacific Ocean to be an area with isotopically heavy benzene. Isotopic compositions tend to be heavier during summer than winter, and the steep gradients of isotopic composition in the Northern Hemisphere equatorial region are more distinctive during winter. There are no published observations of the isotopic composition of atmospheric benzene that are suitable for a comparison with a global model.

3.4. Isotopic Composition and Mean Photochemical Age

[32] Since the OH radical preferentially reacts with unlabeled NMHC, as a compound undergoes photochemical processing in the atmosphere the ratio [^{13}HC]/[HC] will increase. Therefore the amount of change in this ratio (or δ_s-δ_a) can be used to determine the extent of photochemical processing the compound has undergone. The extent of photochemical processing can be considered to be the accumulated amount of OH the compound has experienced since emission, or the time integrated [OH]. In a simplified manner,

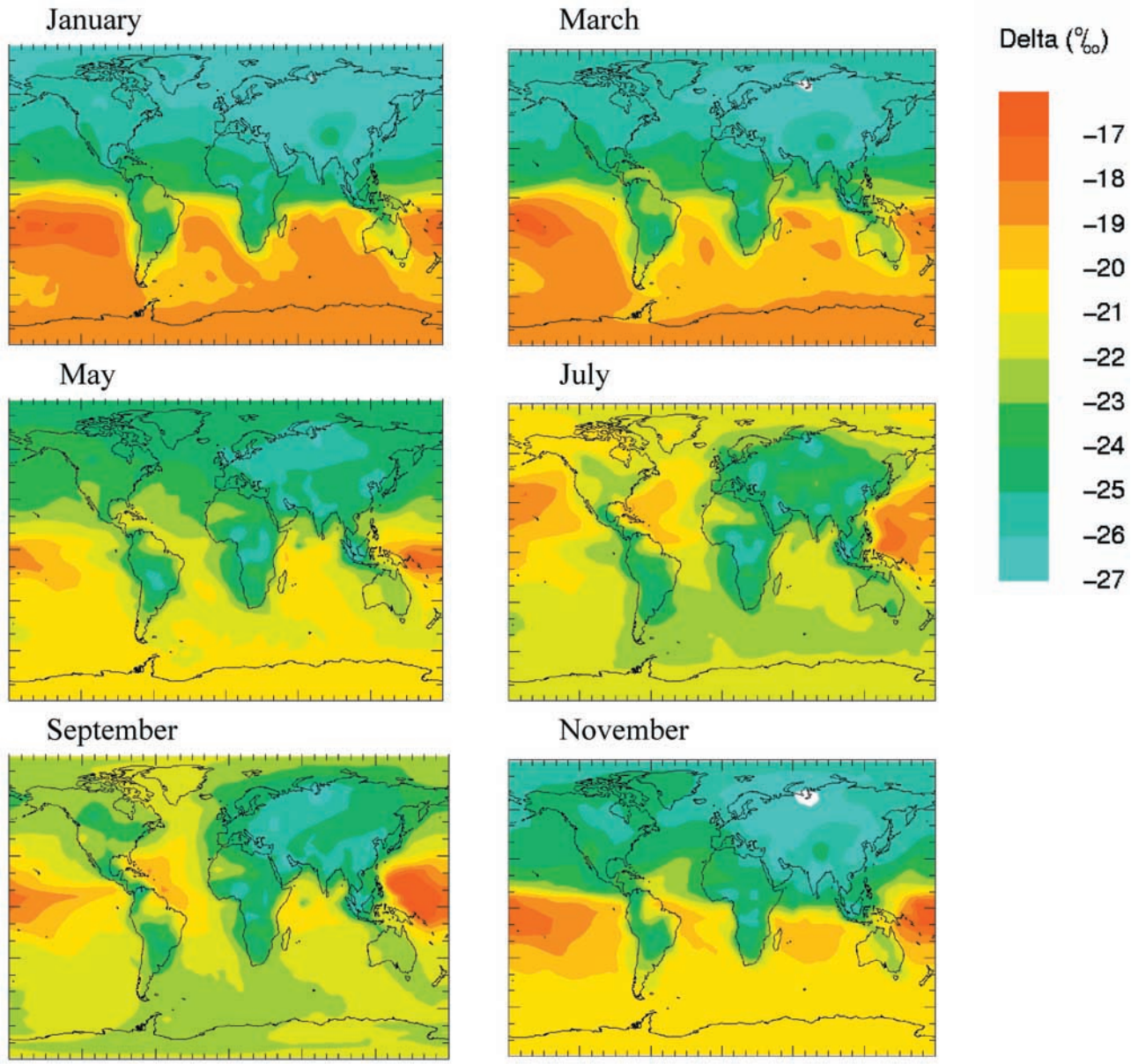

Figure 7. Global distribution of the isotopic composition of ethane, shown as monthly average.

the time integrated [OH] can be expressed as the average amount of time that has passed since emission t_{av}, multiplied by the average $[OH]_{av}$, equation (5).

$$\int [OH]dt = t_{av} * [OH]_{av}. \quad (5)$$

[33] We refer to the average extent of photochemical processing as the "mean photochemical age." *Rudolph and Czuba* [2000] showed that this mean photochemical age of a compound in an air mass can be expressed as a function of δ_s-δ_a, k_{OH}, and ε_{OH} (equation (6)).

$$t_{av} * [OH]_{av} = (\delta_s - \delta_a)/(k_{OH} * \varepsilon_{OH}) \quad (6)$$

It was shown by *Rudolph and Czuba* [2000] that the average photochemical age as calculated from δ_s-δ_a is a

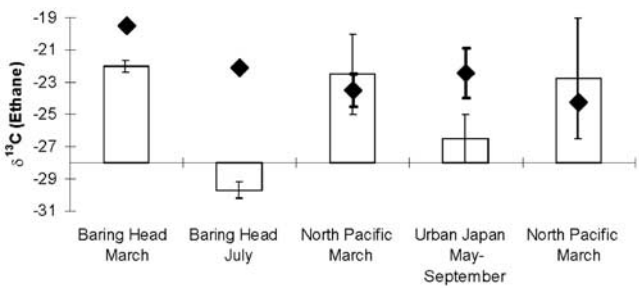

Figure 8. Isotopic measurements of ambient atmospheric ethane (bars, ±1 SD) and corresponding model results (black diamonds, ±1 SD). Y axis intersection is δ_s used in the model.

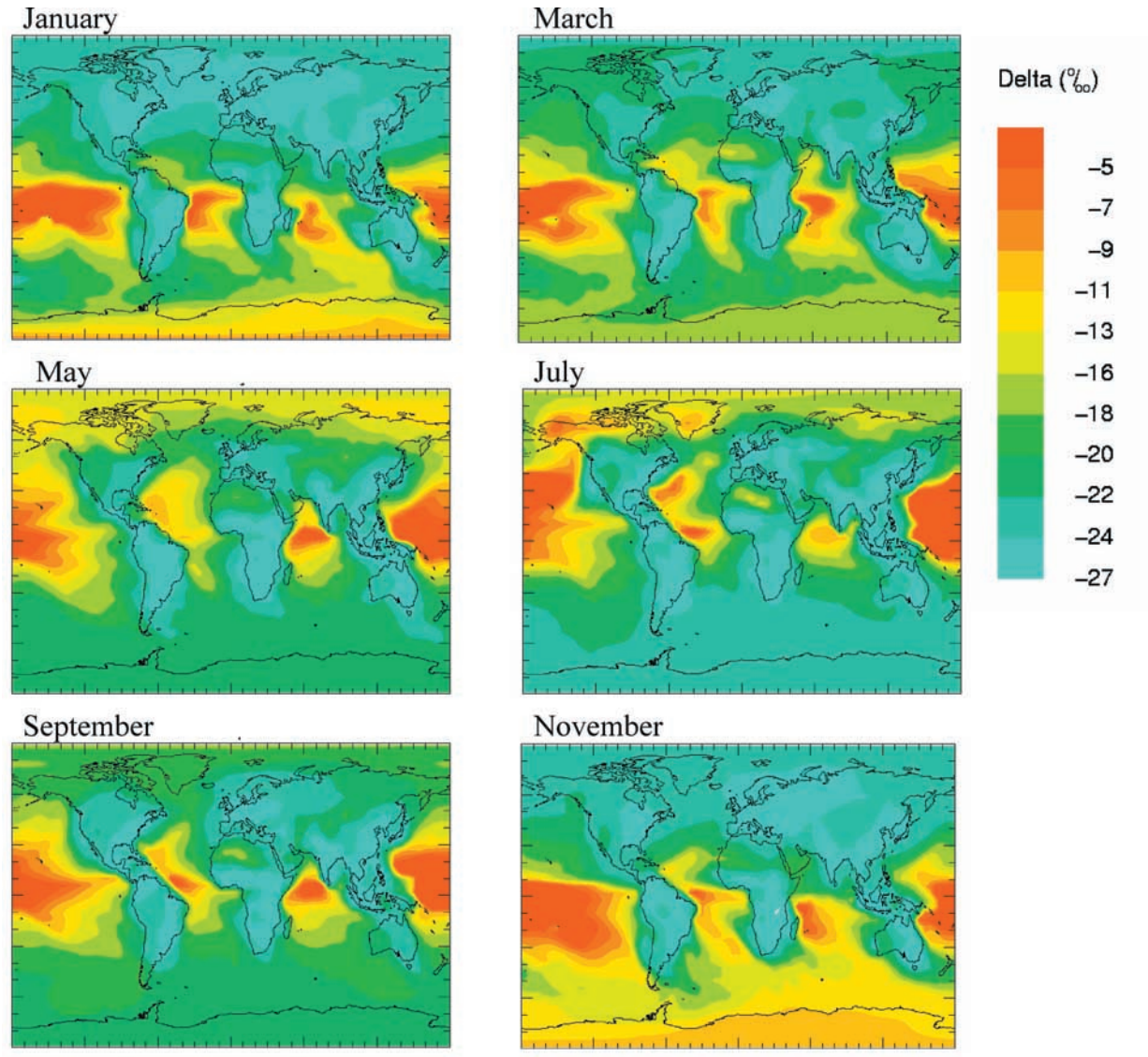

Figure 9. Global distribution of the isotopic composition of benzene, shown as monthly average.

linear weighted average of the ages of the compound in the air mass.

[34] Implicit in this relation is knowledge of the average temperatures the compound has experienced since emission, owing to the temperature dependence of k_{OH} and ε_{OH}. As previously mentioned the temperature dependence of ε_{OH} is negligible within the relevant ambient temperature range. The rate constant, k_{OH}, changes up to 22% for ethane and 5% for benzene within a 30° range of ambient temperatures. Clearly, assuming an average temperature, and therefore an average k_{OH}, introduces some uncertainty. However, if we determine the ratio of mean photochemical age to the average lifetime (τ, equation (7)) the temperature dependence of k_{OH} is to some extent removed.

$$\tau = 1/\left(k_{OH,av} * [OH]_{av}\right), \tag{7}$$

where $k_{OH,av}$ is the rate constant at the average temperature. Rearranging equation (6) we obtain equation (8):

$$t_{av}/\tau = (\delta_s - \delta_a)/\varepsilon_{OH}. \tag{8}$$

It is important to note that the mean photochemical age determined from δ_s-δ_a applies to the studied compound and is not necessarily the age of the air mass.

3.5. Mean Photochemical Age and Concentration

[35] The dependence between observed or modeled concentration for any given location and season, the strength and geographical distribution of the sources, atmospheric transport, and atmospheric removal processes is very complex. Similarly, the average photochemical age represents a complex interaction between transport time, atmospheric removal rates, and mixing of different air masses. When looking at results from high latitudes, the situation is somewhat simplified. NMHC emission rates at high latitudes are very small and in winter the atmospheric lifetimes of NMHC, which are determined by the OH-radical concentration, are very long. Under these conditions we expect that it will be easier to understand the relationship between concentration and mean photochemical age. Atmospheric lifetimes vary greatly with season, latitude, and compound (Table 2). We therefore expect that the relationship between

Table 2. Atmospheric Lifetime (Weeks) of Ethane and Benzene for Different Latitudes at Ground Level[a]

	Ethane				Benzene			
Latitude	January	April	July	October	January	April	July	October
84 N	>1 year	>1 year	>1 year	>1 year	>1 year	47	3.7	>1 year
60 N	>1 year	17	10	>1 year	>1 year	3.7	2.3	18
28 N	15	5.2	5.1	6.8	3.3	1.1	1.1	1.5
4 N	9.2	8.4	6.3	1.5	2	1.8	1.4	3.2
28 S	6.1	8.1	14	7	1.3	1.8	3.1	1.5
60 S	21	>1 year	>1 year	24	4.7	35	>1 year	5.2
84 S	>1 year	>1 year	>1 year	>1 year	>1 year	>1 year	>1 year	>1 year

[a]The calculations are based on the OH-radical concentrations of *Spivakovsky et al.* [2000] and rate constants of 2.57×10^{-13} $cm^3 molecules^{-1} s^{-1}$ for ethane [*Atkinson*, 1994] and 1.18×10^{-12} $cm^3 molecules^{-1} s^{-1}$ for benzene [*Semadeui et al.*, 1995].

concentration and stable carbon isotope ratio will be different for different seasons.

[36] For this reason we selected Alert, Canada (82.5°N, 63.3°W) and the South Pole for a more detailed study of the dependence between stable carbon isotope ratio and concentrations of NMHC. The selection is somewhat arbitrary, but it presents a good example of different regimes, specifically the contrast between seasons when the impact of photochemical loss is more pronounced than the impact of emissions and vice versa.

3.5.1. Ethane at Alert

[37] A plot of ethane concentration versus mean photochemical age at Alert for the period of one year (Figure 10) reveals a striking, systematic seasonal pattern. The lowest concentration and highest stable carbon isotope ratios are observed in summer, consistent with substantial photochemical processing. The highest concentrations are found in winter, coinciding with stable carbon isotope ratios close to the source composition, agreeing with our expectation of marginal chemical processing of ethane in winter. The seasonal change occurs in two distinct regimes. From April to July the concentrations decrease and the photochemical age of ethane increases roughly proportionally to the logarithm of the concentration. Between September and December the concentration increases and the photochemical age decreases, but the shape of the concentration-stable carbon isotope ratio dependence is different.

[38] For an isolated air mass undergoing photochemical processing, the change of isotopic composition is related to the change in concentration via the Rayleigh equation (equation (9)):

$$\delta_t = \varepsilon_{OH} * \ln\left(\frac{[HC]_0}{[HC]_t}\right) + \delta_0, \tag{9}$$

where δ_0 and $[HC]_0$ are the initial isotopic composition and concentration, and δ_t and $[HC]_t$ are the isotopic composition and concentration at time t. The Rayleigh curve for ethane (ε_{OH} = 5‰) is shown in Figure 10. From May until halfway through July the Rayleigh curve provides an excellent fit to the model results (R^2 = 0.99). Given that the Rayleigh approximation assumes the air mass is isolated, the decrease in concentration going into summer must be due to the increase in sunlight and resulting destruction via OH, rather than dilution processes. In other words, the photochemical loss rate is greater than the impact of emissions and transport.

[39] On the other hand, we can describe the period of concentration increase, i.e., during September to December by using a simple relationship describing an ongoing addition process to an air mass, very similar to a standard two-endpoint mixing behavior (dotted line in Figure 10). Air mass A, with a composition corresponding to early August, has the concentration $[HC]_A$ and isotopic composition δ_A. The second air mass B has an isotopic composition of δ_B. Assuming a linear dilution of A with B as the only process influencing concentration and stable carbon isotope ratio, the isotopic composition at time t is a function of the concentration at time t, $[HC]_t$:

$$\delta_t = \frac{[HC]_A * \delta_A + \left([HC]_t - [HC]_A\right) * \delta_B}{[HC]_t}. \tag{10}$$

While identifying the parameters $[HC]_A$, δ_A, and $[HC]_t$ for a data set is trivial, determining δ_B is not. We chose δ_B to give the closest fit to the model results. As δ_B reflects the average photochemical age of the diluting air mass, it is itself a useful parameter.

[40] This approximation for ethane is shown in Figure 10, with $\delta_B = \delta_s$ (−28‰). For this period there is very good agreement between this approximation and the model predictions, R^2 = 0.99. Thus the observed dependence between concentration and stable carbon isotope ratios at high northern latitudes between August and November can be explained by mixing of an atmospheric reservoir of photochemically aged ethane with unprocessed emissions. Although the isotopic information does not allow direct identification of the source region of ethane, the latitudinal concentration gradient (Figure 2) suggests that emissions at

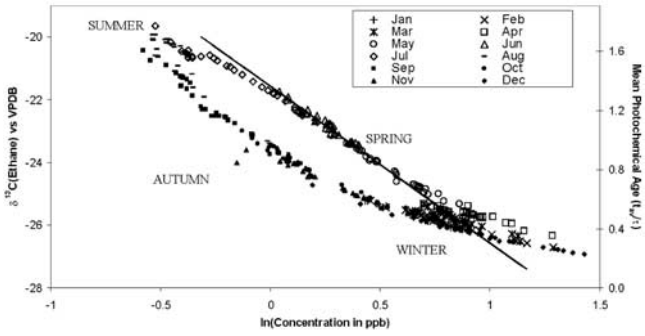

Figure 10. Isotopic composition, mean photochemical age, and concentration of ethane at Alert. Points show daily averages.

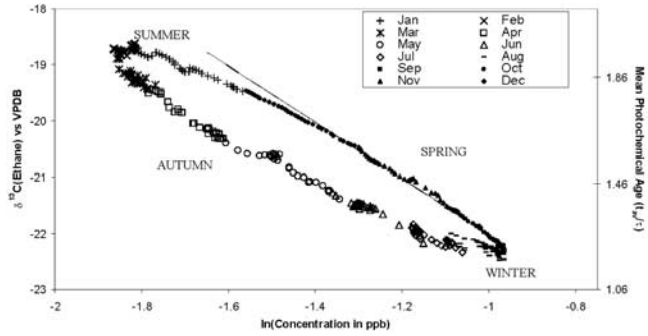

Figure 11. Isotopic composition, mean photochemical age, and concentration of ethane at the South Pole. Points show daily averages.

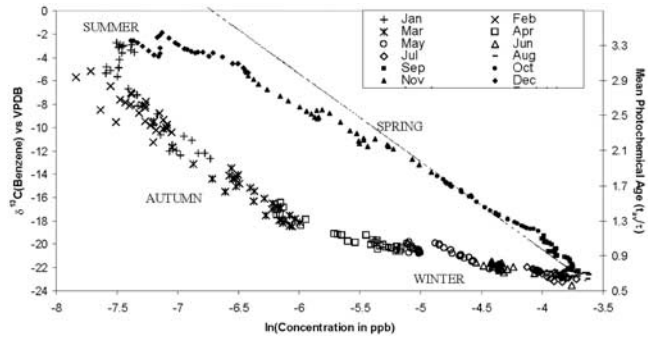

Figure 13. Isotopic composition, mean photochemical age, and concentration of benzene at the South Pole. Points show daily averages.

middle to northern latitudes are driving these changes. In contrast to the April to July period, from September until December the rate of emission of ethane is greater than the photochemical loss rate.

[41] Although the two difference regimes are clearly distinguishable, it is obvious that there are deviations from these idealized curves, especially in the transition phases between the two regimes. During the winter-spring transition period, March and April, chemical processing already has a visible, but not dominant, impact on the stable carbon isotope ratio. Similarly, for part of July and early August the impact of emissions starts to be visible. Later in the year, as the OH-radical concentrations at middle and high northern latitudes decrease, the dominance of the emissions over loss becomes more and more apparent.

3.5.2. Ethane at the South Pole

[42] The dependence between concentration and mean photochemical age for ethane at the South Pole shows features very similar to those seen at Alert (Figure 11). It is not surprising that there is a shift of 6 months i.e., the concentrations and stable carbon isotope ratios decrease between February and August and increase from November to January. The dependence between concentration and stable carbon isotope ratio can be described by the same functions used for Alert. Nevertheless, there are some significant differences. The concentrations are an order of magnitude lower, and the mean photochemical ages almost twice as long as at Alert. The isotopic composition of the second air mass, δ_B, required to fit the function to the results during the Autumn concentration increase (see above) is −25‰, 3‰ heavier than the source composition. Finally, the high, apparently unsystematic wintertime variability of the ethane concentration at Alert is not seen at the South Pole (relative standard deviations of 24% and 7% respectively). These differences are fully consistent with the extreme remoteness of the South Pole, the lower source strength for ethane in the Southern Hemisphere, and the relative proximity of Alert to major sources of ethane.

3.5.3. Benzene

[43] Despite the large difference in atmospheric lifetimes, qualitatively the dependence between concentrations and stable carbon isotope ratios of benzene at Alert (Figure 12) and the South Pole (Figure 13) are very similar to that for ethane. However, there are also significant differences. There is considerably more seemingly random variability in the mean age and concentration of benzene at Alert, particularly at low concentrations. This can be explained by the shorter atmospheric lifetime of benzene, which allows for less averaging. This is also consistent with the lower variability found at the South Pole since the remoteness of Antarctica prevents any direct impact of regional or local sources. The model results for April to June show a weaker dependence between concentration and stable carbon isotope ratio than predicted for a photochemical loss dominated regime. This is most likely due to the impact of regional

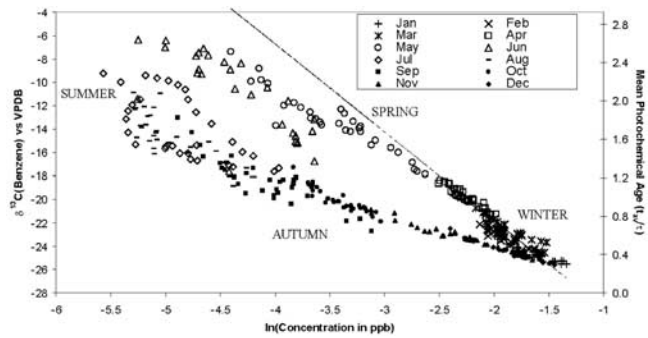

Figure 12. Isotopic composition, mean photochemical age, and concentration of benzene at Alert. Points show daily averages.

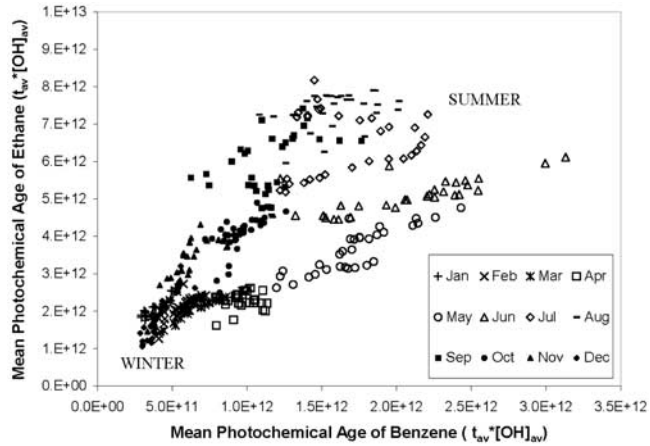

Figure 14. Mean photochemical ages of ethane and benzene at Alert. Points show daily averages.

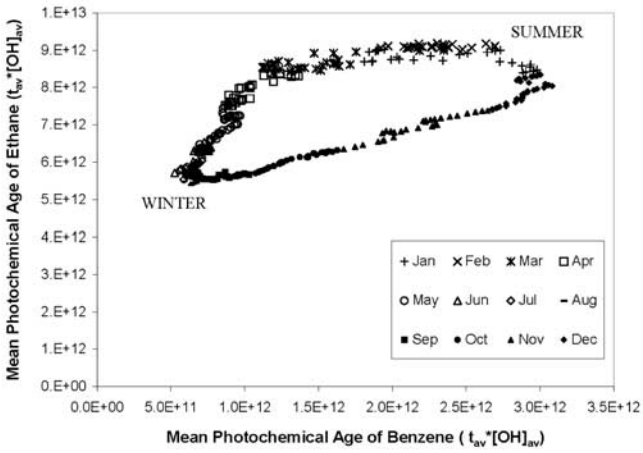

Figure 15. Mean photochemical ages of ethane and benzene at the South Pole. Points show daily averages.

emissions, which becomes more and more apparent with increasing reactivity of the NMHC. The atmospheric lifetime of benzene is about a factor of five shorter than that of ethane (Table 2) and the atmospheric concentration decrease owing to chemical reaction will be much faster resulting in a lower contribution from long range transport to the locally observed concentrations. Indeed, over the last months of spring the model predicts a change by factor of 2–3 in the atmospheric ethane concentration, for benzene more than an order of magnitude. Therefore it is not surprising that for benzene the impact of emissions is more pronounced and can be seen earlier in summer than in the case of ethane.

3.6. Species Specificity of the Mean Photochemical Age

[44] As mentioned above, the mean photochemical age derived from δ_s-δ_a only applies to a single chemical species and not necessarily to the air mass or other trace gases in the studied air mass. Indeed, mean photochemical ages determined from different species in the same air mass are not necessarily consistent. For example, lifetime differences cause concentrations of different NMHC in the remote atmosphere to reflect emissions and processes for differing spatial and temporal scales. Consequently, the mean photochemical age of different species in the same air mass often will be different.

[45] The transition period between regimes with dominance of photochemical loss and dominance of emissions is shifted toward earlier in the year with increasing reactivity. For example marginal photochemical aging of ethane occurs at Alert, meaning the timescales of photochemical processing are larger than those for transport to Alert. However, in the case of benzene in summer local photochemical processing becomes important.

[46] The relationship between mean photochemical ages of ethane and benzene are shown at Alert and the South Pole (Figures 14 and 15). Although more apparent at the South Pole, seasonal variations are evident at both locations. During the months of concentration decrease (i.e., April until June at Alert and October until December at the South Pole) the mean photochemical age of benzene increases approximately linearly with the mean photochemical age of ethane, more or less in accordance with a regime where photochemical loss dominates over the impact of emissions. With the onset of summer, the ethane mean photochemical age continues to increase, while the mean photochemical age of benzene decreases. In summer the concentration of benzene at Alert and the South Pole are very low. Therefore the mean photochemical age of benzene will be very sensitive to the impact of air masses containing low concentrations of less aged benzene. However, the lifetime of ethane is sufficiently long to ensure non negligible concentrations of ethane in background air masses, even at the South Pole. The scatter in the age-age plot for Alert (Figure 14) is due to the relative proximity to major sources.

4. Conclusions

[47] In the study of the isotopic composition of NMHC, the simplicity (and in particular the linearity) of the dependence of the stable carbon isotope ratio and the mean photochemical age has important consequences. Firstly, the mean photochemical age is independent of the source composition. As long as the assumption of a uniform δ_s holds the model can be used to predict changes of mean age and isotopic variability, even without knowledge of the source composition or the source strengths. If there is significant variability of δ_s over time or space, this will result in increased variability in ambient isotopic composition.

[48] The striking seasonal pattern of I^{2}CTM results at Alert and the South Pole for both benzene and ethane illustrates how stable carbon isotopic compositions of atmospheric NMHC can be used to differentiate between photochemical aging and mixing processes in the atmosphere. The model allows the identification of regimes where the isotopic composition is sensitive to particular source types and/or locations. Observations in these areas may be used to identify deficiencies of emission data. For example, if observation and corresponding modeled isotopic composition agree but the concentrations do not, it is likely that the total strength of the sources is unrealistic, rather than the location of the sources in the database. If the isotopic composition of model and observation disagree, regardless of the concentration, the location of sources and relative strengths are in question.

[49] The wide range of lifetimes of NMHC allows for study of atmospheric processing on a range of temporal and spatial scales. Current methodology requires at least 0.5 ng C to measure the isotopic ratio of an atmospheric species to within ±0.5‰ [*Rudolph et al.*, 1997]. In an aged air mass only a few NMHC are present in sufficient concentration to be measured. However, with the developing methodology to measure the stable carbon isotopic composition of atmospheric NMHC at low concentrations, the use of isotopic compositions promises to be an important tool in atmospheric science.

[50] **Acknowledgments.** The authors thank Allen Goldstein for his helpful comments. Alexandra Thompson gratefully acknowledges the American Association for University Women for an International Fellowship during this work. This research was funded by the Natural Science and Engineering Research Council of Canada and the German Minister for Science, Research, Education, and Technology (Förderkennzeichen 01SF9955 and 07ATF39).

References

Atkinson, R., Gas-phase tropospheric chemistry of organic compounds, *J. Phys. Chem. Ref. Data Monogr.*, *2*, 1–216, 1994.

Blake, D., N. Blake, T. Smith, O. Wingenter, and F. Rowland, Nonmethane hydrocarbon and halocarbon distributions during Atlantic Stratocumulus Transition Experiment/Marine Aerosol and Gas Exchange, June 1992, *J. Geophys. Res.*, *101*, 4501–4514, 1996.

Blake, N., D. Blake, T.-Y. Chen, J. Collins, G. Sachse, B. Anderson, and S. Rowland, Distribution and seasonality of selected hydrocarbons and halocarbons over the western Pacific basin during PEM-West A and PEM-West B, *J. Geophys. Res.*, *102*, 28,315–28,331, 1997.

Boudries, H., G. Toupance, and A. Dutot, Seasonal variation of atmospheric nonmethane hydrocarbons on the western coast of Brittany, France, *Atmos. Environ.*, *28*, 1095–1112, 1994.

Boutton, T., *Carbon Isotope Techniques*, edited by D. Coleman and B. Fry, pp. 173–185, Academic, San Diego, Calif., 1991.

Clarkson, T., R. Martin, J. Rudolph, and B. Graham, Benzene and toluene in New Zealand air, *Atmos. Environ.*, *30*, 569–577, 1996.

Ehhalt, D., *Global Aspects of Atmospheric Chemistry*, edited by H. Baumgartel et al., pp. 40–41, Springer-Verlag, New York, 1999.

Fuex, A., The use of stable carbon isotopes in hydrocarbon exploration, *J. Geochem. Explor.*, *7*, 155–188, 1977.

Gautrois, M., Untersuchung organischer Spurengase in der Troposphaere: Globale Verteilungen, jahreszeitliche Variationen und langfristige Trends, Ph.D. thesis, Gerhard-Mercator Univ., Duisburg, Germany, 1999.

Goldstein, A. H., S. C. Wofsy, and C. M. Spivakovsky, Seasonal variations of nonmethane hydrocarbons in rural New England: Constraints on OH concentrations in northern midlatitudes, *J. Geophys. Res.*, *100*, 21,023–21,033, 1995.

Greenberg, J., and P. Zimmerman, Nonmethane hydrocarbons in remote tropical, continental and maritime atmospheres, *J. Geophys. Res.*, *89*, 4767–4778, 1984.

Greenberg, J., P. Zimmerman, and P. Haagenson, Tropospheric hydrocarbons and CO profiles over the U.S. west coast and Alaska, *J. Geophys. Res.*, *95*, 14,015–14,026, 1990.

Hansen, J., G. Russel, D. Rind, P. Stone, A. Lacis, S. Lebedeff, R. Ruedy, and L. Travis, Efficient three-dimensional global models for climate studies: Models I and II, *Mon. Weather Rev.*, *111*, 609–662, 1983.

Jenden, P., and I. Kaplan, Composition of microbial gases from the Middle America Trench and Scipps Submarine Canyon: Implications for the origin of natural gas, *Appl. Geochem.*, *1*, 631–646, 1986.

Kraus, A., F. Rohrer, E. Grobler, and D. Ehhalt, The global tropospheric distribution of NOx estimated by a three-dimensional chemical tracer model, *J. Geophys. Res.*, *101*, 18,587–18,604, 1996.

Laurila, T., and H. Hakola, Seasonal cycle of C2–C5 hydrocarbons over the Baltic sea and northern Finland, *Atmos. Environ.*, *30*, 1597–1607, 1996.

Lobert, J., W. Keene, J. Logan, and R. Yevich, Global chlorine emissions from biomass burning: Reactive chlorine emissions inventory, *J. Geophys Res.*, *104*, 8373–8389, 1999.

McKeen, S., M. Trainer, E. Hsie, R. Tallamraju, and S. Liu, On the indirect determination of atmospheric OH radical concentrations from reactive hydrocarbon measurements, *J. Geophys. Res.*, *95*, 7493–7500, 1990.

McKeen, S., S. Liu, E. Hsie, X. Lin, J. Bradshaw, S. Symth, G. Gregory, and D. Blake, Hydrocarbon ratios during PEM-WEST A: A model perspective, *J. Geophys. Res.*, *101*, 2087–2109, 1996.

McKenna, D., Analytic solution of reaction diffusion equations and implications for the concept of an air parcel, *J. Geophys Res.*, *102*, 19,719–19,725, 1997.

McKenna, D., C. Hord, and J. Kent, Hydroxyl radical concentrations and Kuwait oil fire emission rates for March 1991, *J. Geophys. Res.*, *100*, 26,005–26,026, 1995.

Olivier, J., A. Bouwman, C. Van der Maas, J. Berdowski, C. Veldt, J. Bloos, A. Visschedijk, P. Zandveld, and J. Haverlag, Description of EDGAR version 2.0: A set of global emissions inventories of greenhouse gases and ozone depleting substances for all anthropogenic and most natural sources on a per country basis and on 1° × 1° grid, *RIVM Rep. 771060 002, TNO-MEP Rep. R96/119*, Natl. Inst. of Public Health and the Environ., Bilthoven, Netherlands, 1996.

Parrish, D. D., C. J. Hahn, E. J. Williams, R. B. Norton, F. C. Fehsenfeld, H. Singh, J. D. Shetter, B. W. Gandrud, and B. A. Ridley, Indications of photochemical histories of Pacific air masses from measurements of atmospheric trace species at Point Arena, California, *J. Geophys. Res.*, *97*, 15,883–15,901, 1992.

Penkett, S., N. Blake, P. Lightman, A. Marsh, P. Anwyl, and G. Bitcher, The seasonal variation of nonmethane hydrocarbons in the free troposphere over the north Atlantic ocean: Possible evidence for extensive reaction of hydrocarbons with nitrate radical, *J. Geophys. Res.*, *97*, 2865–2885, 1993.

Prather, M., M. McElroy, S. Wofsy, G. Russell, and D. Rind, Chemistry of the global troposphere: Fluorocarbons as tracers of air motion, *J. Geophys. Res.*, *92*, 6579–6613, 1987.

Roberts, J., F. Fehsenfeld, S. Liu, M. Bollinger, C. Hahn, D. Albritton, and R. Sievers, Measurements of aromatic hydrocarbon ratios and NOx concentrations in the rural troposphere: Observation of air mass photochemical ageing and NOx removal, *Atmos. Environ.*, *18*, 2421–2432, 1984.

Rudolph, J., The tropospheric distribution and budget of ethane, *J. Geophys. Res.*, *100*, 11,369–11,381, 1995.

Rudolph, J., and E. Czuba, On the use of isotopic composition measurement of volatile organic compounds to determine the "photochemical age" of an air mass, *Geophys. Res. Lett.*, *27*, 3865–3868, 2000.

Rudolph, J., and F. Johnen, Measurements of light atmospheric hydrocarbons over the Atlantic in regions of low biological activity, *J. Geophys. Res.*, *95*, 20,583–20,591, 1990.

Rudolph, J., D. Lowe, R. Martin, and T. Clarkson, A novel method of compound specific determination of $\delta^{13}C$ in volatile organic compounds at ppt levels in ambient air, *Geophys. Res. Lett.*, *24*, 659–662, 1997.

Rudolph, J., E. Czuba, and L. Huang, The stable carbon isotope fractionation for reactions of selected hydrocarbons with OH-radicals and its relevance for atmospheric chemistry, *J. Geophys. Res.*, *105*, 29,329–29,346, 2000.

Rudolph, J., E. Czuba, A. L. Norman, L. Huang, and D. Ernst, Stable isotope composition of nonmethane hydrocarbons in emissions from transportation related sources and atmospheric observations in an urban atmosphere, *Atmos. Environ.*, *36*, 1173–1181, 2002.

Saito, T., U. Tsunogai, K. Kawamura, T. Nakatsuka, and N. Yoshida, Stable carbon isotopic compositions of light hydrocarbons over the western North Pacific and implication for their photochemical ages, *J. Geophys. Res.*, *107*(D4), 4040, doi:10.1029/2000JD000127, 2002.

Saueressig, G., J. Crowley, P. Bergamaschi, C. Bruelh, C. Brenninkmeijer, and H. Fischer, Carbon 13 and D kinetic isotope effect in the reactions of CH_4 with O(1D) and OH: New laboratory measurements and their implications for the isotopic composition of stratospheric methane, *J. Geophys. Res.*, *106*, 23,127–23,138, 2001.

Semadeui, M., D. Stocker, and J. Kerr, The temperature dependence of the OH radical reactions of some aromatic compounds under simulated tropospheric conditions, *Int. J. Chem. Kinetics*, *27*, 287–304, 1995.

Singh, H., et al., Impact of biomass burning emissions on the composition of the south Atlantic troposphere: Reactive nitrogen and ozone, *J. Geophys. Res.*, *101*, 23,219–24,203, 1996.

Spivakovsky, C., et al., Three dimensional climatological distribution of tropospheric OH: Update and evaluation, *J. Geophys. Res.*, *105*, 8931–8980, 2000.

Tsunogai, U., N. Yoshida, and T. Gamo, Carbon isotopic compositions of C_2–C_5 hydrocarbons and methyl chloride in urban, coastal, and marine atmospheres over the western North Pacific, *J. Geophys. Res.*, *104*, 16,033–16,039, 1999.

von Czapiewski, K., E. Czuba, L. Huang, D. Ernst, A. L. Norman, R. Koppman, and J. Rudolph, Isotopic composition of non methane hydrocarbons in emissions from biomass burning, *Atmos. Chem.*, *43*, 45–60, 2003.

Yeh, H.-W., and S. Epstein, Hydrogen and carbon isotopes of petroleum and related organic matter, *Geochim. Cosmochim. Acta.*, *45*, 753–762, 1981.

F. Rohrer and O. Stein, ICG II, Troposphere, Forschungszentrum Juelich, D-54825 Juelich, Germany. (f.rohrer@fz-juelich.de; o.stein@fz-juelich.de)

J. Rudolph and A. Thompson, Centre for Atmospheric Chemistry, Chemistry Department, York University, 4700 Keele St., Toronto, ON M3J 1P3, Canada. (rudolphj@yorku.ca; alex_thompsonnz@yahoo.com)